Fig. 1. 2-D slice of a CT volume dataset. The applied contrast agent provides a high vessel-to-tissue contrast and reveals the highlighted portal vein and some branches of the hepatic vein. The two dark spots inside the liver represent liver metastasis. (Dataset provided by Prof. Galanski, Medical School Hannover.)

accuracy of these methods based on studies of corrosion casts of eight human livers.

4) *Vessel visualization*: Based on the skeletons and the information concerning the vessel diameter, antialiased vessel visualizations are generated by fitting graphics primitives along the skeleton lines.

Finally, an interactive 3-D visualization is provided which allows the user to explore the previously identified and analyzed structures. The following sections describe these steps.

II. Medical Background

Because of the complex vascular anatomy of the liver, surgical interventions are challenging. Four different vessel systems supply and drain the liver: the portal vein, hepatic vein, hepatic artery, and bilary ducts. A successful operation requires enough remaining liver tissue supplied by all four vessel systems. Since the portal vein, the hepatic artery, and the bile ducts parallel, the portal vein is regarded as the leading structure for these three vessel systems.

For a surgeon, it is difficult to mentally construct the 3-D structure of vessel systems based on planar slices of radiological data (cf. Fig. 1) and to estimate which part of a vessel system would be damaged as a consequence of a surgical intervention [22]. In order to enable surgeons to perform liver resections respecting the vascular anatomy, a schematic model of the liver was introduced by Couinaud [4]. Following this model, the human liver can be divided into different *segments* which are determined according to the branching structure of the portal vein. A liver segment is defined by the supplied territory of a third-order branch of the portal vein. Since these segments are independent from each other, they can be resected without damaging the supply of the other segments. Applying the widespread scheme of Couinaud directly is questionable from an anatomical point of view, since the liver segments are highly variable in shape, size, and number (see Fasel *et al.* [11]). Therefore, it is desirable to identify the individual liver segments preoperatively.

III. Methods

A. Fast and Robust Vessel Segmentation

The segmentation of the intrahepatic vessels is a prerequisite for a subsequent geometrical and structural analysis. In a preprocessing step, filter functions for noise reduction (Gaussian, median filter) and for background compensation (Laplace-like filters) are applied to the CT data [42]. For background compensation, the size of the filter kernel is chosen such that it is larger than the thickest vessel inside the liver (default is 15×15). The application of this filter is restricted to an interval which is defined such that the lower interval bound roughly corresponds to the gray value of the liver parenchyma and the upper bound corresponds to the brightest values inside the liver.

As a result, intrahepatic vessels can be identified and delineated by using a threshold-based region-growing method. Usually, region-growing segmentation must be repeated with modified thresholds until an appropriate result is found. To accelerate this procedure, we refined the procedure to automatically suggest a threshold.

Initially, a seed voxel of the portal vein close to its entrance into the liver is selected interactively. Starting with this seed voxel, the region-oriented segmentation algorithm iteratively accumulates the 26 adjacent voxels with an intensity equal to or greater than the intensity θ_{beg} of the seed voxel and keeps them in a list $L(\theta_{\mathrm{beg}})$. Using $L(\theta_{\mathrm{beg}})$ as new seed voxels, all adjacent voxels with intensities greater than or equal to $\theta_{\mathrm{beg}} - 1$ are collected in a list $L(\theta_{\mathrm{beg}} - 1)$. The threshold is further decreased until a given threshold θ_{end} is reached which definitively creates only voxels $L(\theta_{\mathrm{end}})$ outside the vessel systems.

The generation of the voxel lists is performed efficiently because voxel lists for the segmentation with threshold $\theta - 1$ have already been constructed when using the threshold θ. In total, some 100 lists are generated which takes approximately 3–5 s on modern PC hardware for high-resolution CT datasets (512×512 matrix with slice distance 3 mm).

The automatic threshold selection is based on the observation that the number of voxels $N(\theta)$ is approximately linear decreasing for $\theta = \theta_{\mathrm{opt}} \cdots \theta_{\mathrm{beg}}$ (Fig. 2). At θ_{opt}, the slope changes considerably because many voxels belonging to the liver tissue are collected for thresholds below θ_{opt}. Thus, a suggestion for θ_{opt} can be found by calculating an optimal fit of two straight lines for $N(\theta)$. For this purpose, the two characteristic parts of the curve are approximated by two regression lines. The points $(\theta_{\mathrm{beg}}, |N(\theta_{\mathrm{beg}})|) \cdots (j, |N(j)|)$, respectively, $(j+1, |N(j+1)|) \cdots (\theta_{\mathrm{end}}, |N(\theta_{\mathrm{end}})|)$ are employed to calculate the correlation coefficients for both lines. j is chosen such that the sum of the two correlation coefficients is maximal.

We found that the position of the crossing of both regression lines yields a good suggestion for θ_{opt} in most cases. If the suggested threshold is not satisfying, it may be changed interactively. On the basis of the generated voxel lists $L(\theta_{\mathrm{beg}}) \cdots L(\theta_{\mathrm{end}})$, the vessel system specified by any threshold θ can be displayed very fast by simply drawing all precalculated voxels from the lists $L(\theta_{\mathrm{beg}}) \cdots L(\theta)$.

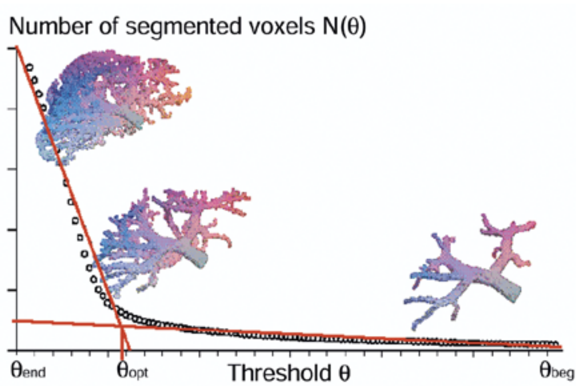

Fig. 2. Estimation of an optimal threshold for vessel segmentation. (©Springer 2000, originally published in [43], reprinted with permission.)

B. Graph-Based Analysis of Vasculature

The segmentation result is a set of voxels representing the intrahepatic vessel systems. For surgery planning, a further analysis of these voxels is required. This includes geometric measurements of the branches (radius, length) and the identification of the ramification pattern (e.g., to determine the main portal subtrees supplying the liver segments).

Before the analysis of the vessel systems is carried out, a segmentation problem due to imaging artifacts has to be approached. Depending on the scanning protocol, usually two or more different vessel systems of the liver are enhanced with contrast agent during the scan. Often the portal and hepatic vein are affected, which are shown in Fig. 3(a). Therefore, the scan yields high-intensity voxels for both vessel systems. Due to the limited spatial resolution of the scanned volume data, voxels of different vessel systems are often adjacent to each other such that they are segmented as one object when in reality there is only proximity between the two. A manual separation of the different vessel systems would be too time consuming for clinical routine. Therefore, we analyze and separate such "forests" of connected vessel systems automatically using graph theoretical methods. In a first step, the voxel-based shape representation of the vessels is transformed into an abstract graph representation, utilizing "skeletonization." The skeleton representation carries all information about the original shape of the object and, at the same time, facilitates an algorithmic geometrical and structural shape analysis. The principal approach is illustrated in Fig. 4.

1) Skeletonization: The skeleton, or medial axis in two dimensions (2-D), of an object in continuous 2-D space is defined as the set of all points which are equidistant from at least two points on the boundary of the object [3]. In discrete space, this definition cannot be applied directly. Since the discretization generally produces jagged surfaces, many irrelevant skeleton branches would arise. We use "thinning" as a basic technique for the skeletonization and, thus, successively erode the surface voxels of an object, until the skeleton remains. During this process, three aspects are crucial to preserve the properties of continuous skeletons and to yield skeletons which reflect the original shape of the vessel system.

1) The erosion of the voxels must not change the topology of the original structure, i.e., the number of connected objects, cavities, and 3-D holes must remain the same.

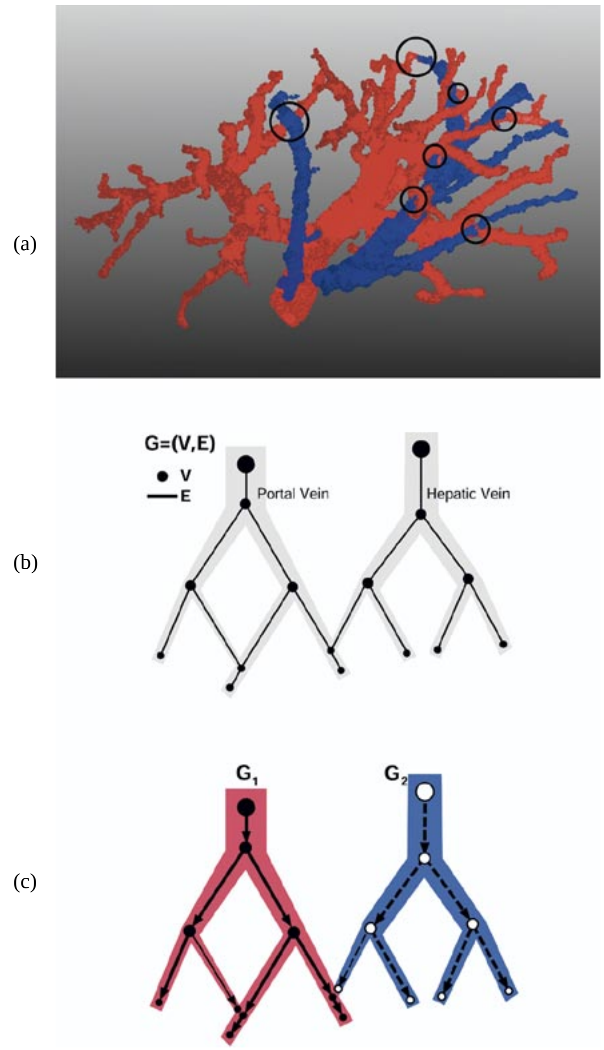

Fig. 3. (a) Portal vein (red) and fragments of the hepatic vein (blue) as result of the vessel segmentation based on an underlying CT examination, in which both vessel systems are enhanced with contrast agent. Both systems touch at the encircled points of contact and cannot be segmented separately. (b) Graph G of two touching vessel systems. (c) Orientation of G, which consists of directed acyclic graphs G_1 and G_2. (©Springer 2000, originally published in [43], reprinted with permission.)

2) The erosion must be carried out symmetrically to provide a reliable and accurate central position of the skeleton.
3) Noisy vessel surfaces should not lead to "irrelevant" skeleton lines, which would be mistakenly interpreted as side branches.

Although many 2-D skeletonization algorithms have been developed for applications ranging from optical character recognition to biological cell studies (see, e.g., [21] for a survey), relatively few methods exist for the 3-D case (see Section V-D).

In our skeletonization approach, it is checked for each voxel whether its deletion preserves the 3-D topology of the object. Voxels with this feature are called *simple points* [19] and only these are deleted in the erosion process. Efficient methods to detect simple points are described, e.g., by Davies and Lee [6], [23].

To cope with anisotropic voxels, special care of a precise symmetric erosion was required. Therefore, we combined the skeletonization with a distance transformation and introduced a